

QUARTERLY JOURNAL
OF THE
ROYAL METEOROLOGICAL SOCIETY

Vol. 128

JANUARY 2002 Part A

No. 579

Q. J. R. Meteorol. Soc. (2002), **128**, pp. 1–23

The response of the coupled tropical ocean–atmosphere to westerly wind bursts

By ALEXEY V. FEDOROV*
Princeton University, USA

(Received 21 December 2000; revised 15 June 2001)

SUMMARY

Two different perspectives on El Niño are dominant in the literature: it is viewed either as one phase of a continual southern oscillation (SO), or alternatively as the transient response to the sudden onset of westerly wind bursts (WWBs). Occasionally those bursts do indeed have a substantial effect on the SO—the unusual strength of El Niño of 1997/98 appears to be related to a sequence of bursts—but frequently the bursts have little or no impact. What processes cause some bursts to be important, while others remain insignificant? The question is addressed by using a simple coupled tropical ocean–atmosphere model that simulates a continual, possibly attenuating, oscillation to study the response to WWBs. The results show that the impact of WWBs depends crucially on two factors: (i) the background state of the system as described by the mean depth of the thermocline and intensity of the mean winds, and (ii) the timing of the bursts with respect to the phase of the SO. Changes in the background conditions alter the sensitivity of the system, so that the impact of the bursts on El Niño may be larger during some decades than others. Changes in the timing of WWBs affect the magnitude and other characteristics of the SO by modifying the energetics of the ocean–atmosphere interactions. A reasonable analogy is a swinging pendulum subject to modest blows at random times—those blows can either magnify or diminish the amplitude, depending on their timing. It is demonstrated that a WWB can increase the strength of El Niño significantly, if it occurs 6 to 10 months before the peak of warming, or can reduce the intensity of the subsequent El Niño, if it occurs during the cold phase of the continual SO.

KEYWORDS: El Niño–Southern Oscillation Intraseasonal variability Madden–Julian oscillation Ocean–atmosphere interactions Predictability

1. INTRODUCTION

What causes the southern oscillation (SO)†, which has El Niño as its warm phase and La Niña as its cold phase, to be irregular and thus difficult to predict? Why does its period vary from roughly 3 to 6 years? Why did the events of 1982 and 1997 have such exceptional amplitudes? Why was the event of 1992 so prolonged? The list of questions is extensive, and different investigators propose different processes to answer these questions. The explanations include: tropical ocean–atmosphere interactions sufficiently unstable to bring into play nonlinearities, thus generating chaotic behaviour (Cane *et al.* 1986); interactions between the interannual oscillation and the seasonal cycle (Tziperman *et al.* 1995; Chang *et al.* 1995; Jin *et al.* 1996); random atmospheric disturbances, or the atmospheric ‘noise’ (Penland and Sardeshmukh 1995; Blanke *et al.* 1997; Wunsch 1999; Thompson and Battisti 2000); and the decadal modulation of the interannual oscillation because of gradual changes in the background state (Fedorov

* Corresponding address: Atmospheric and Oceanic Sciences Program, Department of Geosciences, Princeton University, Sayre Hall, PO Box CN710, Princeton, NJ 08544, USA. e-mail: alexey@splash.princeton.edu

† This phenomenon is often referred to as El Niño–Southern Oscillation (ENSO); however, here the name southern oscillation is used to emphasize that both El Niño and La Niña are two equally important phases of this oscillation.

© Royal Meteorological Society, 2002.

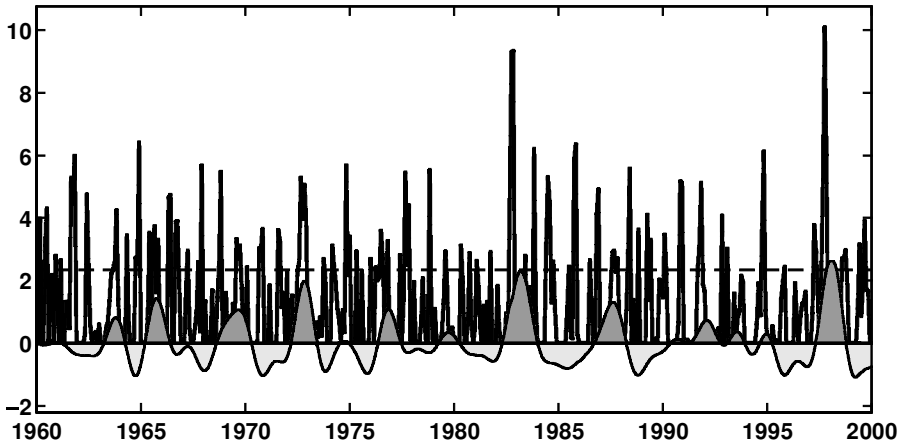


Figure 1. Westerly wind bursts as seen in the higher-frequency variations of the zonal wind stress (in units of 0.02 dyn cm^{-2}) averaged in the domain 145°E – 210°E , 5°S – 5°N from available observations. The lower-frequency component of the signal, corresponding to periods longer than 12 months, is subtracted from the record, while the negative values (i.e. easterly wind bursts) are not shown. The dashed line corresponds to the mean-square amplitude of the westerly bursts. The underlying plot shows the interannual changes in the Niño-3 sea surface temperature (SST) (in degC). Different climatologies, for the periods of 1960–80 and 1980–2000, respectively, were used to calculate SST anomalies during those two periods. Note that some of the wind fluctuations shown in the figure may be due to the wind relaxation caused by El Niño. Also, because of the use of monthly data, the shorter wind bursts are not recorded.

and Philander 2000, 2001). In reality, several of these processes can contribute to the irregularity of the SO, so that each needs to be explored separately. This paper concentrates on the effect of westerly wind bursts (WWBs).

Although possible causes of the WWBs are still being debated, the most frequently cited is the active phase of the so-called Madden–Julian oscillation, or MJO (Madden and Julian 1972, 1994; Woolnough *et al.* 2000). Tropical cyclones and other mesoscale phenomena (Harrison and Vecchi 1997) can also lead to westerly wind events but of somewhat shorter duration. The WWB can appear annually, usually during the early calendar months of the year when the prevailing trade winds relax, and sometimes briefly reverse their direction. The duration of such wind events varies from roughly a week to about two months, with the strongest anomalous winds developing in the western Pacific. A wind burst is sometimes an isolated event, sometimes a sequence of episodes.

Figure 1 shows the magnitude of the high-frequency surface westerly winds in the western equatorial Pacific calculated by spatially averaging available data since 1960 (mostly from the COADS*) in the vicinity of the date-line. These results, obtained by using monthly winds, are basically consistent with those reported by Slingo *et al.* (1999) for MJO activity based on NCEP/NCAR† re-analysed data. Still, while there is general agreement between the results in Fig. 1 and their work, there are some differences. For instance, Slingo *et al.* use the variance of the upper-tropospheric zonal velocity (as well as other variables) band-passed in the 20 to 100-day interval as an MJO index, which is different from, although related to, the strength of surface WWBs. Further, Slingo’s analysis suggests that the MJO activity may have increased after the mid-1970s, while the present analysis shows a relatively uniform level of the bursts throughout the record.

* Comprehensive Ocean–Atmosphere Data Set.

† National Centers for Environmental Prediction/National Center for Atmospheric Research.

In spite of these and some other differences, Fig. 1 serves as a fairly good illustration of the WWB activity throughout the last 40 years.

Numerous studies concern the dynamical response of strictly the ocean to WWBs that generate mainly Kelvin waves (Philander 1981; Harrison and Giese 1988; Giese and Harrison 1991; Kindle and Phoebus 1995; McPhaden and Yu 1999). The effect of the WWBs on the coupled system has been explored in connection with the generation of El Niño from a state of rest, to activate an SO in coupled ocean–atmosphere models (for example, Zebiak and Cane 1987; Battisti 1988). In these models, as well as in the observations, a WWB generates a downwelling Kelvin wave that propagates along the thermocline to the eastern Pacific (Kessler *et al.* 1995; Hendon and Glick 1997; Hendon *et al.* 1998). The Kelvin wave is accompanied by anomalous surface currents which transport warmer water to the east. These two effects, advection and a deepening of the thermocline, can warm sea surface temperatures (SSTs) in the eastern Pacific Ocean, thus reinforcing the weakening of the trade winds and initiating positive feedbacks that may result in El Niño. Based on a statistical analysis of the tropical winds and SSTs for the period 1986–98, Vecchi and Harrison (2000) estimate that an average WWB is followed by a warming in the eastern and central Pacific of as much as 1 degC. Presumably, developments were along these lines in 1997 (McPhaden 1999; McPhaden and Yu 1999). Figure 1 shows that the wind bursts were particularly intense in 1982 and in 1997 (though this exceptional strength might have been due in part to a wind relaxation caused by El Niño), but those bursts failed to generate El Niño on other occasions (e.g. in 1967 and 1988–89). There have also been occasions (e.g. 1965) when El Niño developed in the absence of any sound WWBs. What conditions determine the impact of WWBs?

The modelling studies mentioned above and some others regard the SO as an initial-value problem. The so-called ‘non-normal mode’ theories (e.g. Farrell and Moore 1992; Moore and Kleeman 1997, 1999) are also related to the initial-value approach, in the sense that a perturbation (perhaps the optimal perturbation) is needed for El Niño to develop. The phenomenon can alternatively be viewed as an eigenvalue problem, as a continual, natural mode of oscillation. Those continual modes are usually governed by some version of the ‘delayed’ (Schopf and Suarez 1988; Battisti and Hirst 1989) or ‘recharge’ oscillator (Jin 1997a,b), in which the continuation of oscillations is provided by the ocean memory* and the positive feedbacks of the ocean–atmosphere interactions. This paper tries to bridge the two different approaches to the SO, i.e. the initial- and eigenvalue approaches, and shows that the one does not exclude the other. Here we study how wind bursts influence the continual SO which is regarded as analogous to the oscillations of a damped pendulum. Noise maintains the oscillations by supplying energy to the system, but is not necessarily essential for each particular event. In the same way that modest blows to a swinging pendulum can sometimes magnify, sometimes diminish, the amplitude of the swing, so WWBs can sometimes have a large effect, sometimes a minimal effect, on the SO. A surprising result that emerges from the analysis is that a WWB close to the peak of the cold event can lower the strength of the following El Niño by reducing the energy of the oscillations. The most intense warm events are found to develop when the burst happens 6 to 10 months before the peak of an imminent El Niño. This may explain the huge amplitude of El Niño in 1982 and 1997.

* The dynamical response of the ocean to changes in the wind includes off-equatorial thermocline anomalies in the central and western Pacific of the opposite sign to those in the eastern Pacific. The off-equatorial anomalies propagate towards the equator, then travel along the thermocline to the eastern Pacific and induce the next phase of the oscillation.

Another factor that influences the response to WWBs is the background or mean state of the ocean–atmosphere system. Recently, Fedorov and Philander (2000, 2001) showed that the characteristics of the SO (the period between events, the growth/decay rates of instabilities, the direction of propagation of the anomalies, etc.) are strongly dependent on the basic state which can be described in terms of the time- and zonally-averaged intensity, τ , of the Pacific trade winds, the mean depth, H , of the thermocline (the layer of large density gradients that separates the warm surface waters from the cold waters at depth), and the temperature difference, ΔT , across the thermocline. The analysis will show that the response of the ocean–atmosphere system to wind bursts is sensitive to changes in the mean state as well. The gradual relaxation of the easterly winds along the equator since the 1970s, and the associated warming of SSTs in the eastern Pacific—all indicators of a changing mean state—could have caused the system to be more sensitive to the wind bursts in the 1980s and 1990s than in the 1960s and 1970s.

2. THE MODEL AND METHODS

The observed spectrum of interannual variability in the tropical Pacific (calculated, for instance, from the SST data in Fig. 1) has a spectral maximum corresponding to the SO at about 3–5 years. The width of the spectral peak is about 4 years so that the relative width, $\Delta\omega/\omega$, of the spectral peak in the frequency domain is $\Delta\omega/\omega \sim 1$. This suggests, but does not rigorously prove, that the system has a natural mode of oscillation that may be slightly damped or neutrally (marginally) stable. (If in a model $\Delta\omega/\omega \ll 1$ then it usually means that the system is unstable, as in the case of the chaotic model of Zebiak and Cane (1987). If $\Delta\omega/\omega \gg 1$ then the system is usually strongly damped, although other factors may contribute to the broadening of the spectrum, such as the mean state modulations altering ω .) How close the observed SO is to neutral stability is a matter that remains unsettled; for a discussion see Thompson and Battisti (2000). For the purpose of this paper, it is assumed that the SO is weakly damped so that oscillations attenuate in the absence of the forcing.

A coupled ocean–atmosphere model similar to those of Zebiak and Cane (1987), Battisti and Hirst (1989) and Jin and Neelin (1993) is used, with adjustable parameters whose values were chosen to ensure simulations in good agreement with observations since the 1980s. The simulated SO corresponds to a weakly damped mode. Once the various parameters have been specified, their values are kept constant except for changes in the values of τ and H which are varied in order to explore different background states. For dynamical consistency, the model determines the oceanic currents, slope of the thermocline, and SST for each mean state. The ocean–atmosphere interactions are included in the model by relating the wind-stress anomalies to the SST anomalies. For simplicity, the asymmetries of the background state and the annual cycle are neglected. A detailed description of the model is given by Fedorov and Philander (2001); also see the appendix.

Two sets of experiments were conducted. In the first set, τ and H are varied and the coupled response of the system to a WWB is studied for different basic states, when the system is initially at rest*. In the second set, the effect of changes in the timing of the WWB with respect to the already existing ENSO cycle is studied. The model wind burst is centred at the equator at about 165°E longitude, and its shape in space and time

* In the ocean there always exists a steady circulation associated with steady winds. The use of the term ‘at rest’ simply means that the system stays in its basic state and no interannual oscillations occur.

is given by a Gaussian function

$$\tau_{\text{wwb}} = \tau_0 \exp\{-(x/L)^2 - (y/Y)^2 - (t/D)^2\}, \quad (2.1)$$

where τ_{wwb} is the anomalous wind stress due to the burst, t is time, and x and y are the longitude and latitude coordinates, respectively. $L = 4000$ km, $Y = 1700$ km, $D = 10$ days, and $\tau_0 = 0.10$ dyn cm⁻² is chosen. Such scale factors L and Y allow one to approximate the shape of a westerly wind composite given by Perigaud and Cassou (2000), time D gives a pulse lasting for about one month, and τ_0 yields a wind burst with the spatially averaged magnitude equal to the mean-square amplitude of the bursts in Fig. 1. Even though the stress given by this Gaussian function is a very idealized representation of the actual wind fluctuations, and other choices of L , Y , D and τ_0 may be possible, the qualitative results of the analysis remain valid for a broad range of parameters and other shapes of the burst. (Moore and Kleeman (1997) studied which spatial structures are especially efficient in forcing their intermediate model.)

Significantly, with the parameters chosen, WWBs of relatively moderate magnitudes can be used. In reality, WWBs with amplitudes two to three times larger and lasting even two months are not that infrequent. One of the controversies surrounding WWBs is that some believe that the momentum from the bursts becomes dispersed over a significant depth instead of staying localized on the thermocline—this indeed happens in some coupled general-circulation models (GCMs), so that wind-forced equatorial Kelvin waves on the thermocline remain too weak to affect SST and to start ocean–atmosphere interactions. In contrast, simple models based on the two-layer description of the ocean tend to transfer all the momentum from the wind into thermocline motion, thereby exaggerating the magnitude of the signal propagating along the thermocline. Until this issue is resolved, using moderate wind bursts allows one to make reasonable conclusions without relying heavily on the actual magnitude of the bursts. Another reason for using moderate wind magnitudes is to avoid strongly-nonlinear atmospheric feedbacks that may be too dependent on their parametrization in simple models.

It should also be emphasized that this study deals with the effect of separate WWBs (perhaps a sequence of WWBs), rather than with the full effect, on the interannual variability in the tropics, of the ‘weather’ or ‘climate noise’ that consists of the superposition of both westerly and easterly wind bursts, and of other disturbances. This latter subject also bears some controversy since some models appear relatively insensitive to such noise (Zebiak 1989), while others respond more strongly to the low-frequency tail of the noise (Roulston and Neelin 2000). Those issues are related to such factors as the relative levels of the noise and the signal (e.g. Chang *et al.* 1996), the spectral composition of the noise, essential nonlinearities, the particular model used, etc. and are not considered in this paper.

A typical response of the system to a single westerly wind pulse is shown in Fig. 2 which depicts changes in the SST in the Niño-3 region. After the burst and some initial adjustment, the system oscillates with some characteristic period determined by the delayed-oscillator physics. In this particular example, the period of the cycle is about 5 years. Note that the behaviour of the coupled system is very different from the ocean-only response with no coupling. (No coupling implies that the SST does not affect the atmosphere, and there is no atmospheric feedback into the ocean through the wind stress. In terms of the coupling coefficient, μ , no coupling means $\mu = 0$, see the appendix.) The ocean–atmosphere interactions effectively prolong and enhance the warming induced by the Kelvin wave and anomalous surface currents, and result in long-period oscillations. Curiously, whereas in the coupled case the warming of the eastern

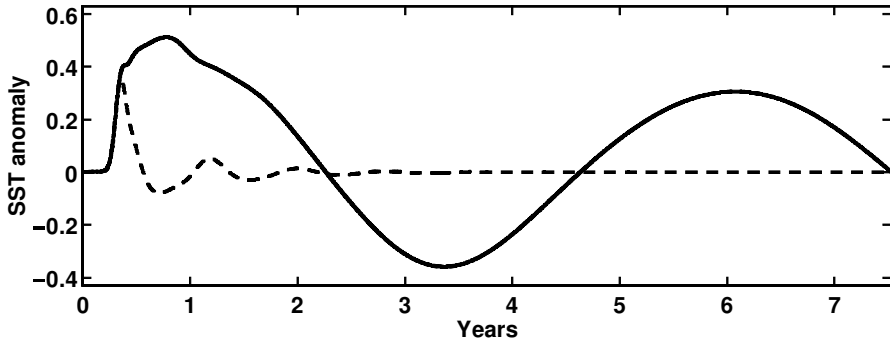


Figure 2. A typical model response of the coupled ocean–atmosphere to a westerly wind burst, as seen in the evolution of the anomalous sea surface temperature (SST) of the Niño-3 region (in degC). The dashed line corresponds to the case when no ocean–atmosphere coupling is allowed. The ocean is initially at rest.

Pacific still persists half a year after the wind burst, in the uncoupled case a weak cooling has already developed by this time.

3. THE OCEAN–ATMOSPHERE RESPONSE: CHANGING THE BACKGROUND STATE

The results in Fig. 3(a) show the maximum anomalous warming in the Niño-3 region, in response to a given wind burst, for different mean states of the coupled system corresponding to different values for H and τ . The wind burst is always the same, and the recorded SST is the maximum value during the next year after the burst. Figure 3(b) shows the results when no coupling is allowed (i.e. $\mu = 0$, see the appendix). The difference is dramatic; the coupling between ocean and atmosphere through SSTs can amplify the response—the warming of the eastern Pacific—by a factor of five.

The strongest response in Fig. 3(a) is achieved when the background state has relatively strong winds and a deep thermocline (in the upper right corner of the figure). For a fixed thermocline depth, there is an optimum value for the winds. To explain these results, let us consider several extreme cases. In the case of weak winds and a deep thermocline, the thermocline is almost flat so that a Kelvin wave forced by a WWB hardly affects the surface in the east, and ocean–atmosphere interactions are inhibited. Next, consider a shallow thermocline and strong winds that cause the thermocline to have a large slope. This creates a strong cold tongue extending far west—a situation relatively stable because a rather strong wind burst is needed to displace the western Pacific warm pool eastward or to change the temperature of the upwelled water in the eastern Pacific. Thus, in these two extreme cases the system is relatively insensitive to the action of WWBs. The sensitivity is huge when the thermocline is deep and the easterly winds are strong because, under such conditions, most of the Pacific Ocean is warm, and there is a strong but relatively small-sized cold tongue in the east. Any disturbance, such as a Kelvin wave induced by a WWB, will immediately lead to the displacement of the warm water farther east, so that the cold tongue will begin to vanish, thereby starting a feedback reaction and further reducing the winds. The large thermocline slope implies that the system has a huge amount of available potential energy (APE) (e.g. Goddard and Philander 2000), release of which contributes to larger growth rates for the instability and higher sensitivity of the system to WWBs.

The diagram in Fig. 3(a) shares similarities with stability diagrams produced by Fedorov and Philander (2000, 2001) on the basis of a linear eigenvalue analysis of

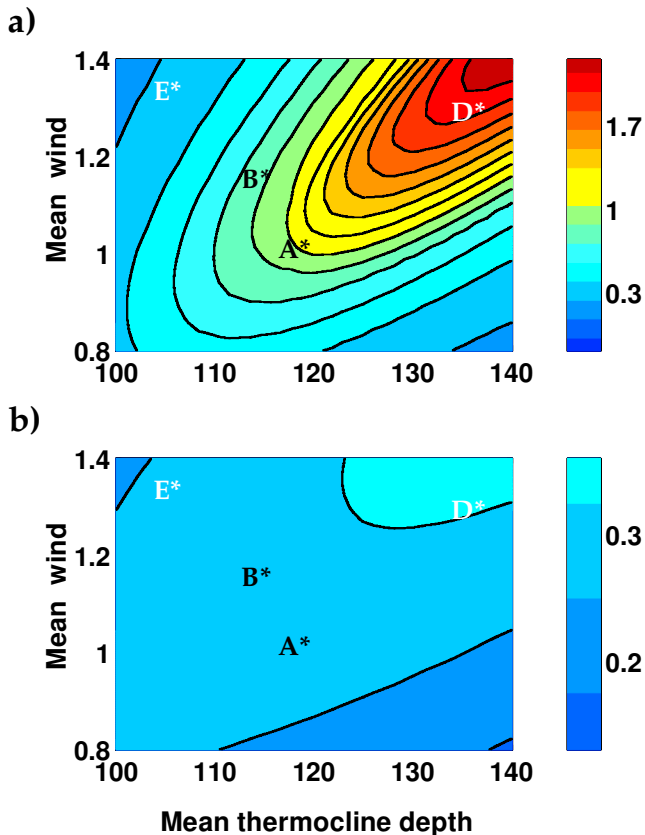


Figure 3. The response of the ocean–atmosphere (in degC), to the same westerly wind burst (WWB), with (a) standard coupling and (b) no coupling, shown as the maximum warming of the eastern Pacific Ocean within the first year after the WWB as a function of changes in the mean easterly winds along the equator, τ , and in the mean depth of the equatorial thermocline, H . For the winds, the unit of 1 corresponds to about 0.5 dyn cm^{-2} ; the thermocline depth is given in metres. To produce each subplot, approximately 500 numerical runs were conducted for different combinations of τ and H . See the text for the significance of points A, B, E, and D.

different mean states (cf. Fig. 4(b) of Fedorov and Philander 2000, the growth rates). Their stability analysis indicates the existence of two main families of unstable modes to which they referred as ‘local’ and ‘remote’ modes—the latter is related to the delayed oscillator. These two families yield two local maxima in the stability diagram for the growth rates. For the local mode, SST variations depend on upwelling and advection induced by local wind fluctuations close to the SST variations in the central and, especially, eastern Pacific Ocean. For the remote mode, they depend on the vertical movements of the thermocline in response to wind fluctuations further west. A shallow thermocline (the proximity of point E, Fig. 3(a)) favours the higher-frequency local mode with a period on the order of 1 year and with westward propagation of the SST anomalies. A deep thermocline (proximity of point D, Fig. 3(a)) favours the low-frequency remote mode with a period on the order of 5 to 10 years and a slightly-eastward propagation of the SST anomalies. For the present conditions in the tropical Pacific, the SO has a hybrid character (in the neighbourhood of points A and B), with some aspects of both families, to a degree that depends on the closeness of a mode to either points E or D in Fig. 3(a).

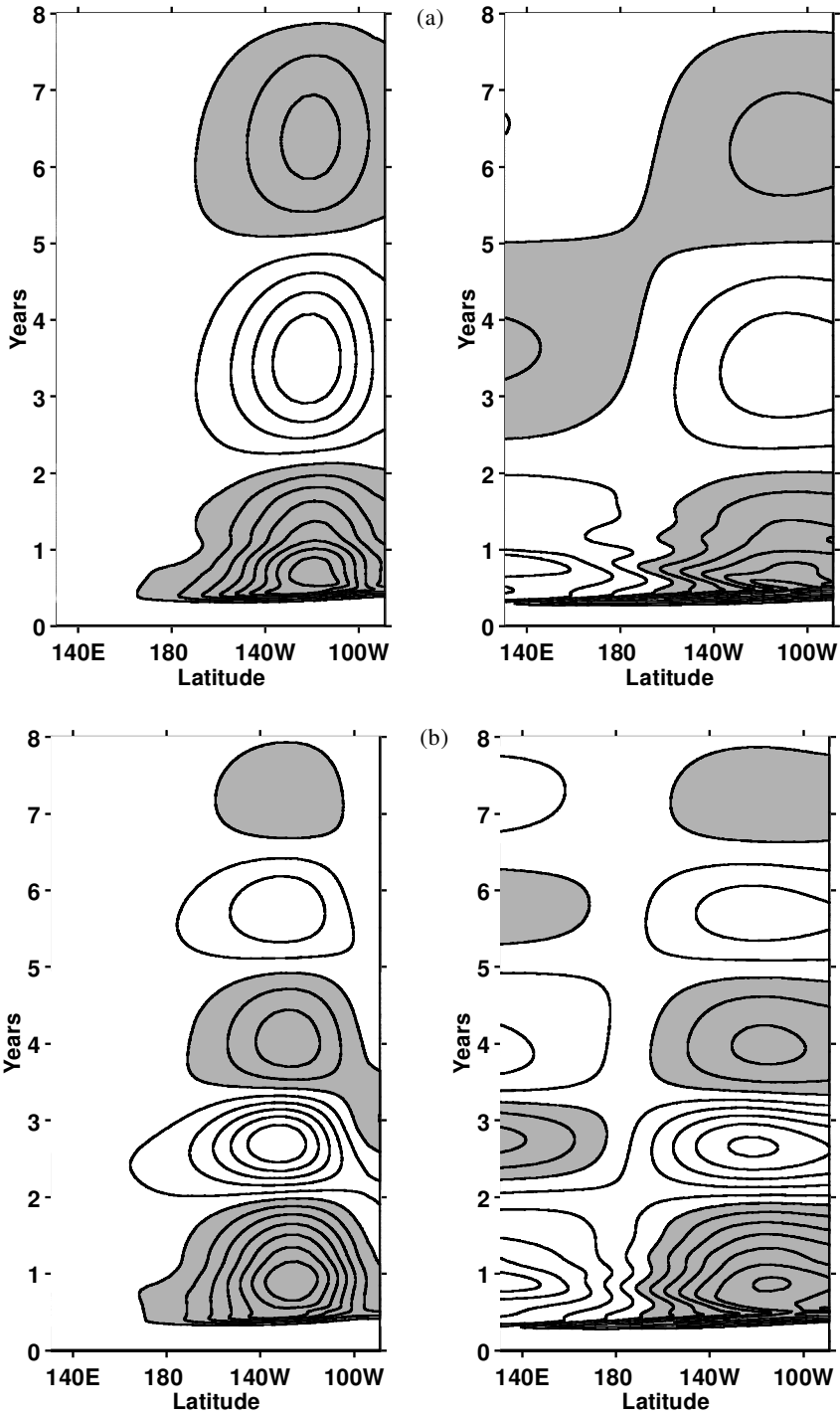


Figure 4. (a) The response of the coupled ocean–atmosphere to a westerly wind burst (WWB), as seen in the evolution of the anomalous sea surface temperatures (SSTs) (the left panel) and the thermocline displacement (the right panel) for the basic state corresponding to point A in Fig. 3. Dark shading indicates warmer SSTs and deeper thermocline. (b) The same as in (a), but the basic state corresponds to point B in Fig. 3. (c) The ocean-only response to a WWB, as seen in the evolution of the anomalous SSTs (the left-side panel) and the thermocline displacement (the right-side panel) for the basic state corresponding to point A in Fig. 3. No ocean–atmosphere coupling is allowed.

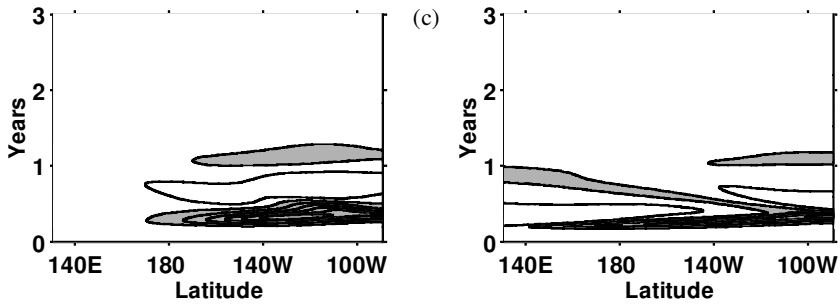


Figure 4. Continued.

Importantly, Fig. 3(a) has only one local maximum, which nearly coincides with the maximum for the remote mode from the linear analysis. There is no maximum in the figure corresponding to the local mode because WWBs can directly excite only the remote mode. Since those winds are confined to the neighbourhood of the date-line, they do not affect upwelling in the eastern Pacific, but influence developments further east ‘remotely’ by their effect on vertical movements of the thermocline. If the background state should move towards point D, then the response to WWBs will increase.

It appears that, since the 1980s, conditions in the tropical Pacific correspond to the vicinity of point A in Fig. 3(a). During the 1960s and 1970s, SST in the east was lower, the zonally-averaged winds were stronger, and the thermocline was shallower in the eastern Pacific, so that conditions were closer to point B. (For a description of the decadal fluctuation see Zhang *et al.* (1997), Guilderson and Schrag (1998), Giese and Carton (1999), and Chao *et al.* (2000)). Figure 3(a) suggests that such a change in background conditions may have caused the response of the coupled ocean–atmosphere to a WWB to be stronger in the 1980s and 1990s than in the 1960s and 1970s.

From a mathematical point of view the effectiveness of WWBs in initiating the coupled oscillations may result from the governing equations being not self-adjoint, and from the perturbations (in the form of WWBs) having a structure similar to (although not in all models) that of the so-called optimal perturbations. A number of studies have explored the ‘non-normal modes’ in the coupled system which are also called transients, or the singular vectors of the propagator matrix (Penland and Sardeshmukh 1995; Moore and Kleeman 1997, 1999; Thompson and Battisti 2000). The growth of a non-normal mode, which is more rapid than the normal-mode analyses would indicate, is evident during the first year in Figs. 4(a) and (b). These figures depict the attenuating oscillations excited by a WWB in the cases of two different background states, those corresponding to points A and B, respectively.

It is important to emphasize that there are actually four time-scales evident in Fig. 2 and in Fig. 4(a) or 4(b). The shortest scale, of order 1 to 2 months, is associated with the ocean crossing time for a Kelvin wave. The medium scale, extending from 6 months to about a year, corresponds to the transient evolution of the initial disturbance in the coupled system. The longer scale corresponds to the period of the natural (normal) oscillations in the system and is about 3 (at point B) to 5 (at point A) years. Finally, the fourth scale is determined by the damping and is chosen here to be on the order of a decade. Air–sea interactions appear to become especially pronounced at the medium and longer time-scales. Consequently, both normal and ‘non-normal’ modes determine the overall dynamics of the coupled ocean–atmosphere.

Note that after the first year, the dominant time-scale is that of the normal mode which has a shorter period in the case of point B than point A, in accord with the linear stability analysis of Fedorov and Philander (2000, 2001). Another effect of the change in background state on the normal mode is different phase propagation of the SST anomalies: it is slightly eastward for the mode at point A, and westward for the mode at point B.

In summary, it has been shown that the effect of the WWBs can be different from one decade to another depending upon background conditions in the tropics. The differences are caused by a number of factors, including changes in the system sensitivity, and changes in the properties of the normal and non-normal modes. This result can explain the observation of Perigaud and Cassou (2000) that a decadal ‘preconditioning’ of the ocean may be necessary for a wind burst to have a significant effect on El Niño. They find that an increase in ocean heat content (OHC) averaged along the equator increases sensitivity. Increased OHC implies a deeper thermocline and movement from point B to A in Fig. 3(a), which explains the greater sensitivity of the system to wind bursts.

Finally, in Fig. 4(c) calculations are presented for the ocean-only response to a WWB, with no coupling allowed ($\mu = 0$). The figure shows the propagation of Kelvin and Rossby waves that are reflected at the eastern and western boundaries. Within half a year to a year of the burst, the original signal almost vanishes because of the strong energy loss at the boundaries. The propagation of the Kelvin wave—actually a part of the initial adjustment of the ocean—is also evident in Figs. 4(a) and 4(b) but, after a few months, ocean–atmosphere interactions rule out a description of the response in terms of separate Kelvin and Rossby waves or their reflections at coasts. Given the results in Fig. 4, it is not surprising that attempts to test the delayed-oscillator theory by directly measuring the reflection of equatorial waves at the boundaries give little evidence of such reflection (Delcroix *et al.* 1994; Kessler and McPhaden 1995; Boulanger and Menkes 1995).

4. OCEAN–ATMOSPHERE RESPONSE: CHANGING THE TIMING OF WIND BURSTS

So far we have considered the impact of the WWBs when the system is at rest. In reality, the ocean is constantly bombarded by various disturbances, including wind bursts, and is also subject to seasonal and much slower decadal changes as discussed earlier. As a result, instead of the relatively simple patterns of Figs. 2 or 4, we will have a complex superposition of different influences leading to the irregular oscillation seen in Fig. 1. This brings us to the next question: what will the impact of a wind burst be when there already exists a continual oscillation? To answer this question we next fix a basic state that resembles conditions in the tropical Pacific at present (point A in Fig. 3), and investigate the response when a WWB happens at different phases of an ongoing continual SO, i.e. a cycle with alternating El Niño and La Niña phases. Before turning attention to the response it is useful to consider the energetics of the system.

Let us define the APE of the oscillations (we will use E for simplicity) as

$$E = \frac{\rho}{2} \iint g'h^2 \, dx \, dy - \frac{\rho}{2} \iint g'\bar{h}^2 \, dx \, dy, \quad (4.1)$$

where g' is the reduced gravity, ρ is the mean water density, and h is the total local depth of the thermocline. Hereafter, except in g' , the bars and primes denote mean (time-averaged) and anomalous values, respectively. The integrals are calculated over the entire domain of the tropical Pacific. (Note that according to the definition used in (4.1), this APE is actually a perturbation APE, and as such can be both positive and

negative.) It can be easily shown that the main balance is between the term on the left and the first term on the right in the following equation (see the appendix, also see Goddard and Philander (2001)):

$$\frac{d}{dt}E = W + (\dots), \quad (4.2)$$

$$W \propto \iint (\bar{u}\tau' + u'\bar{\tau}) dx dy, \quad (4.3)$$

where W is the wind power (i.e. the work being done by the wind per unit time), $\bar{\tau}$ and τ' are the mean and anomalous wind stress, respectively, and \bar{u} and u' are the mean and anomalous velocity at the surface that is related to changes in the thermocline depth (see Eqs. (A.1)–(A.3) of the appendix). The omitted terms in the brackets describe dissipation and energy loss through the boundaries of the basin, and the higher-order nonlinear terms. Those omitted terms may become important during strong El Niño events.

It follows that the energetics involve mainly work done by the wind on the ocean to generate APE. In a continual oscillation, La Niña corresponds to a state of maximum, El Niño to a state of minimum APE. In the absence of dissipation, the wind power is out of phase with APE by a quarter period. In Fig. 5 that oscillation is depicted as the black line which corresponds to a slowly attenuating SO in the absence of any external forcing. The basic state produces weakly-damped decaying oscillations, or ‘ringing’, with a 5-year periodicity, which might be an appropriate description of the sequence of El Niño episodes in 1982, 1987 and 1992. Also shown in Fig. 5 is the impact of a WWB at two different times. A wind burst at a relatively short time before the peak of El Niño is seen to strengthen the warm event. However, if the wind burst happens near the peak of the cold phase it effectively diminishes the strength of the following El Niño. This happens because the wind burst reduces the APE of the oscillations. Such a reduction in the APE prevents a strong El Niño from developing. This may explain why the relatively potent wind bursts of 1988–89 or 1984–85 did not result in El Niño or any significant warming afterwards: the bursts happened during the cold phase of the cycle (see Fig. 1). A simple analogy for this effect is an oscillating pendulum—if the pendulum is hit in its lower position in the direction opposite to the motion, the amplitude of the oscillations diminishes. On the other hand, when a pendulum is hit in the upper position, the amplitude of the oscillations would actually increase.

Figure 6 shows the evolution of the APE and the wind power corresponding to the cases in Fig. 5. On the interannual time-scales the wind burst is very short, almost instantaneous, so that in Fig. 6 the immediate direct effect of the burst appears as a sharp drop in the values of wind power, and as a kink in the energy curve where the derivative dE/dt changes almost instantaneously. Since u' and τ' induced by the burst have the opposite direction with $\bar{\tau}$ and \bar{u} , the wind work produced by WWBs will be negative regardless of the timing of the burst. Thus, if the burst happens when the APE is negative (i.e. during the warm phase of the SO), the wind work increases the absolute values of the APE and amplifies the oscillation. However, if the burst happens when the APE is positive, the work goes toward the reduction of the APE, which weakens the oscillation. This consideration supports our analogy between the coupled ocean–atmosphere system and a pendulum forced by random disturbances.

A plot of E versus W will be a circle in the case of a neutral oscillation, or a spiral in the case of a damped oscillation as seen in Fig. 7. The eccentricity of the spiral is determined by the value of the lag between the wind power and the APE—a smaller

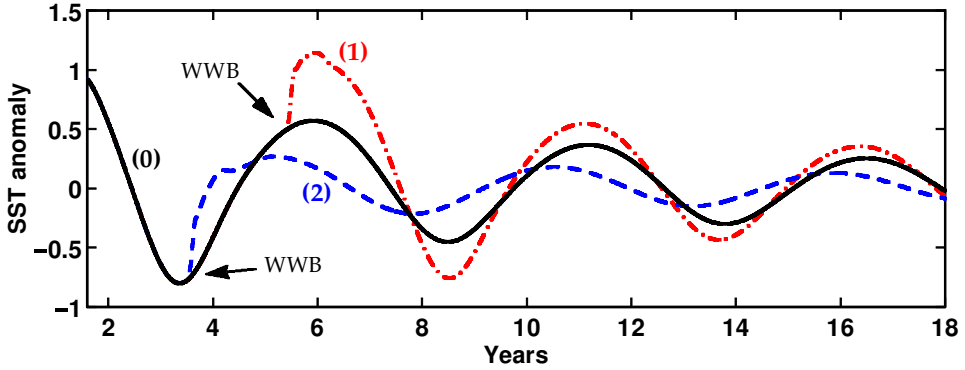


Figure 5. The response of the coupled ocean–atmosphere, with a slowly attenuating southern oscillation, to a westerly wind burst (WWB), as seen in the evolution of the anomalous sea surface temperature (SST) of the eastern Pacific (in degC). (0) The WWB never happens (black continuous line), (1) the burst occurs about 6 months before the peak of El Niño (red dot-dashed line), and (2) the burst occurs 3 months after the peak of La Niña (blue dashed line).

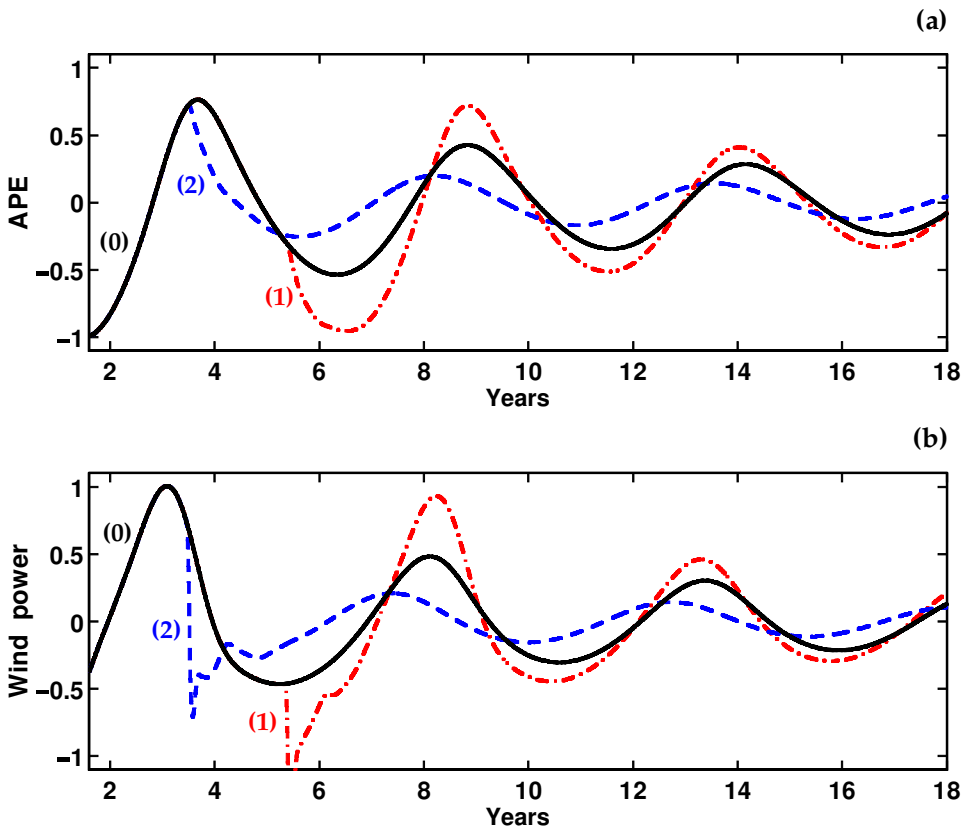


Figure 6. The response of the coupled ocean–atmosphere, with a slowly attenuating southern oscillation, to the same westerly wind burst, as seen in (a) the evolution of the available potential energy (APE) of the system, and (b) the evolution of the wind power. The units of energy and wind power are nondimensionalized. Note that the sea surface temperature of the eastern Pacific and the APE are approximately anti-correlated with a small delay of several months in the APE. (0)-(1)-(2) as in Fig. 5.

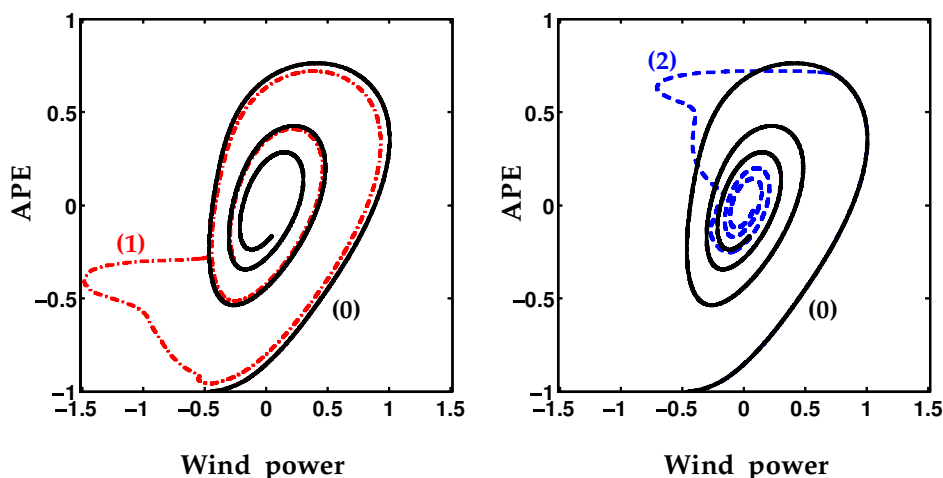


Figure 7. Changes in the phase trajectories of the coupled ocean–atmosphere induced by the same westerly wind bursts (WWBs) as in Figs. 5 and 6. The diagrams of available potential energy (APE) versus wind power are shown. (0)-(1)-(2) as in Fig. 5. In the absence of the bursts, the trajectory of the system follows a slowly converging spiral. One of the effects of the WWBs is to transfer the system onto a higher (1) or lower (2) loop of the spiral (that is, onto a higher or lower phase orbit).

lag implies a larger ratio between the lengths of the main axes of the spiral. A wind burst strongly perturbs the trajectory of the system, so that the trajectory returns to the undisturbed spiral only in another part of the phase space. If it re-approaches the spiral at a lower loop than it was during the burst, the energy of the oscillation is reduced. If the trajectory manages to jump to a higher loop, then the APE is increased.

Changes in the phase space allow estimates of the strength of the wind bursts relative to the magnitude of a continual, i.e. pre-existing, SO. Thus, diagrams similar to those in Fig. 7 can provide a convenient framework for examining the effect of the WWBs not only in simple models, but in complex GCMs as well. A study is under way to apply this approach in the analysis of the effects of WWBs in the data from a realistic GCM forced by the observed winds over the second half of the century.

Additional examples of the impact of WWBs are shown in Figs. 8, 9 and 10. A WWB some time after the peak of El Niño, but still within the warm phase of the SO (line 3), results in the appearance of a secondary peak for El Niño, and a prolongation of the warm event. This may be the explanation for the repeated warming during the period 1992–95 (Trenberth and Hoar 1996; Goddard and Graham 1997, also see Fig. 1). Similarly, the doubled-peaked El Niño of 1969/70 and 1982/83 may reflect the effect of the WWBs.

In the final example, a WWB happens within the cold part of the cycle, but before the peak of La Niña (line 4, Figs. 8, 9 and 10). The result is a weak transient warming in the middle of La Niña. Low temperatures then return and La Niña continues. This may be an explanation for the short-lived warming of the eastern Pacific in 1974 (Fig. 1), which never developed into El Niño. On that occasion the bursts happened too early in the cold phase of the SO, so that La Niña was interrupted but then was able to recover before giving way to the next (but delayed) El Niño.

In summary, there are four different ways in which a WWB can affect a continual SO. Depending on its timing, a burst can (1) amplify the SO, thus increasing the strength

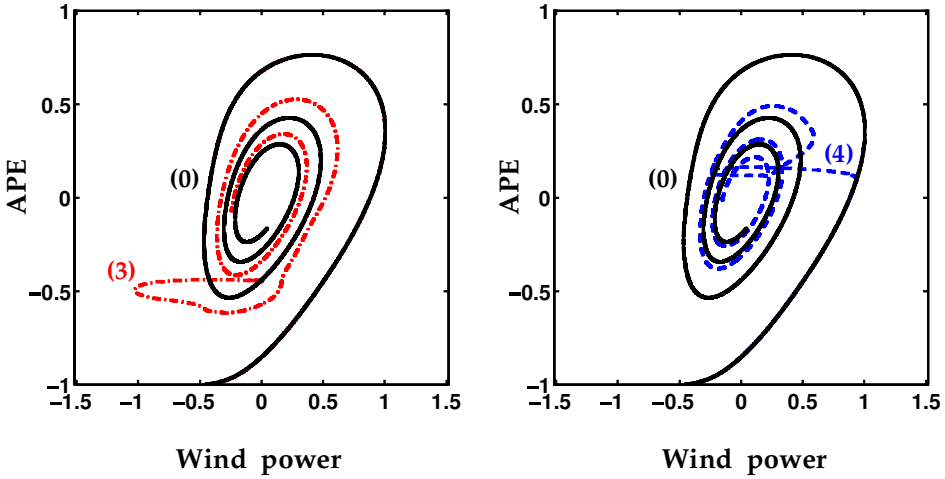


Figure 8. Additional examples of changes in the phase trajectories of the coupled ocean–atmosphere induced by westerly wind bursts (WWBs) with different timings. Despite relatively small changes in the available potential energy (APE) induced by the bursts, one of the effects of WWBs is, nonetheless, to transfer the system onto a higher (3) or lower (4) loop of the spiral. Also note the small loops associated with the direct effect of the bursts. The temporal evolution of sea surface temperature, energy and wind power is shown in Figs. 9 and 10. Further particulars of (0)-(3)-(4) are described in the caption of Fig. 9.

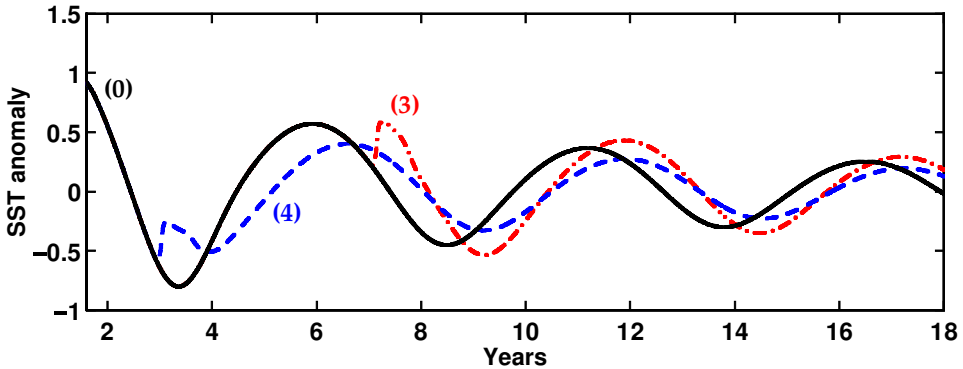


Figure 9. The response of the coupled ocean–atmosphere, with a slowly attenuating southern oscillation, to westerly wind bursts (WWBs), as seen in the evolution of the anomalous sea surface temperature (SST) of the eastern Pacific (in degC). The corresponding phase diagrams are shown in Fig. 8. (0) The WWB never happens (black continuous line), (3) the burst occurs about 9 months after the peak of El Niño, leading to the development of the secondary El Niño maximum (red dot-dashed line), and (4) the burst occurs about 5 months before the peak of La Niña, leading to a weak transient warming in the middle of the cold part of the cycle (blue dashed line).

of El Niño; (2) weaken La Niña and the next El Niño, by reducing the amplitude of the SO; (3) cause a doubled-peaked El Niño, thus increasing the duration of the event; and (4) cause a transient warming during La Niña, delaying the next El Niño.

In cases (2) and (4), a WWB decreases the amplitude of the SO. The shaded parts of the curve in Fig. 11 show during which phases of the oscillation a WWB can induce such a reduction in amplitude. It amounts to a third of the cycle. In reality, the SO is skewed, with La Niña persisting much longer than El Niño so that the period during which WWBs can cause a reduction in amplitude may be even longer.

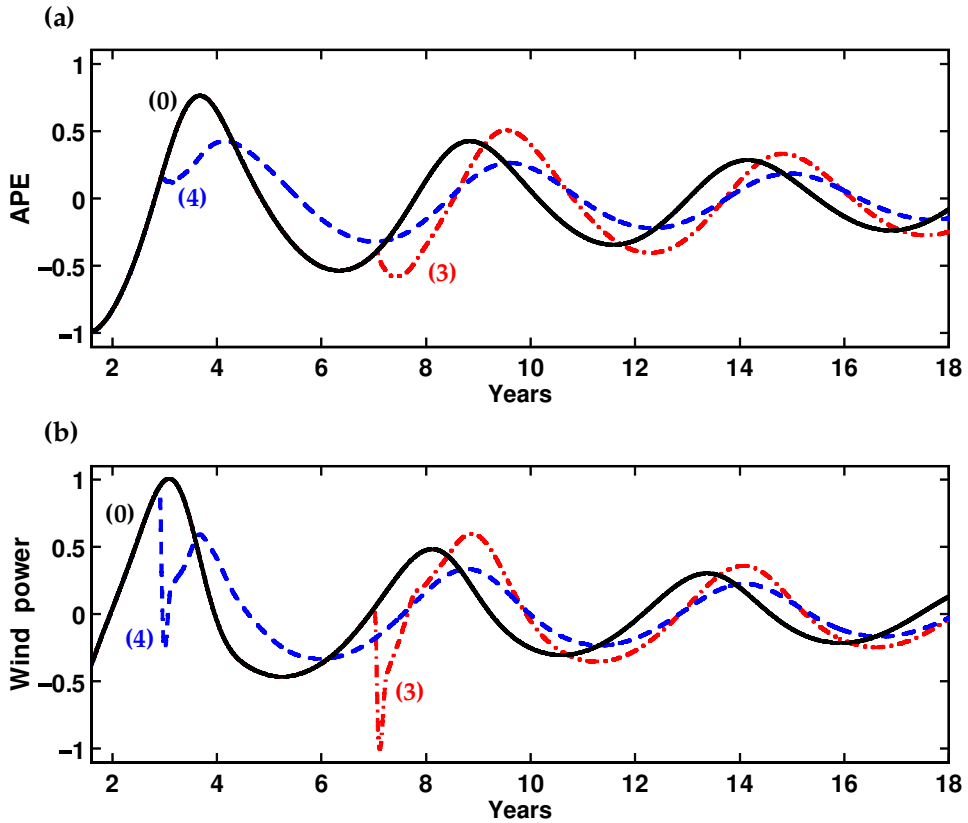


Figure 10. The response of the coupled ocean–atmosphere, with a slowly attenuating southern oscillation, to the same westerly wind burst, as seen in (a) the evolution of the available potential energy of the system, and (b) the evolution of the wind power. The units for energy and wind power are nondimensionalized. (0)-(3)-(4) as in Fig. 9. The corresponding phase diagrams are shown in Fig. 8.

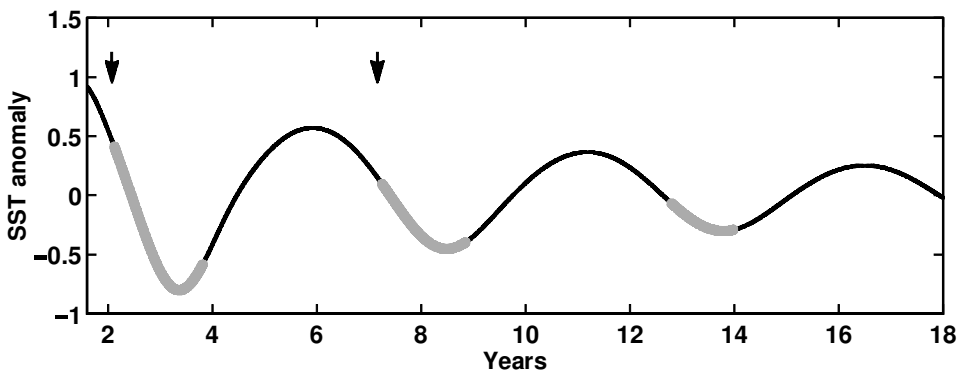


Figure 11. A slowly attenuating southern oscillation as seen in the evolution of the anomalous sea surface temperature (SST) of the eastern Pacific (in degC). The marked segments of the plot correspond to times when a westerly wind burst would reduce the amplitude of the oscillation. The arrows mark the beginning and the end of the cycle used for obtaining the results of Fig. 12.

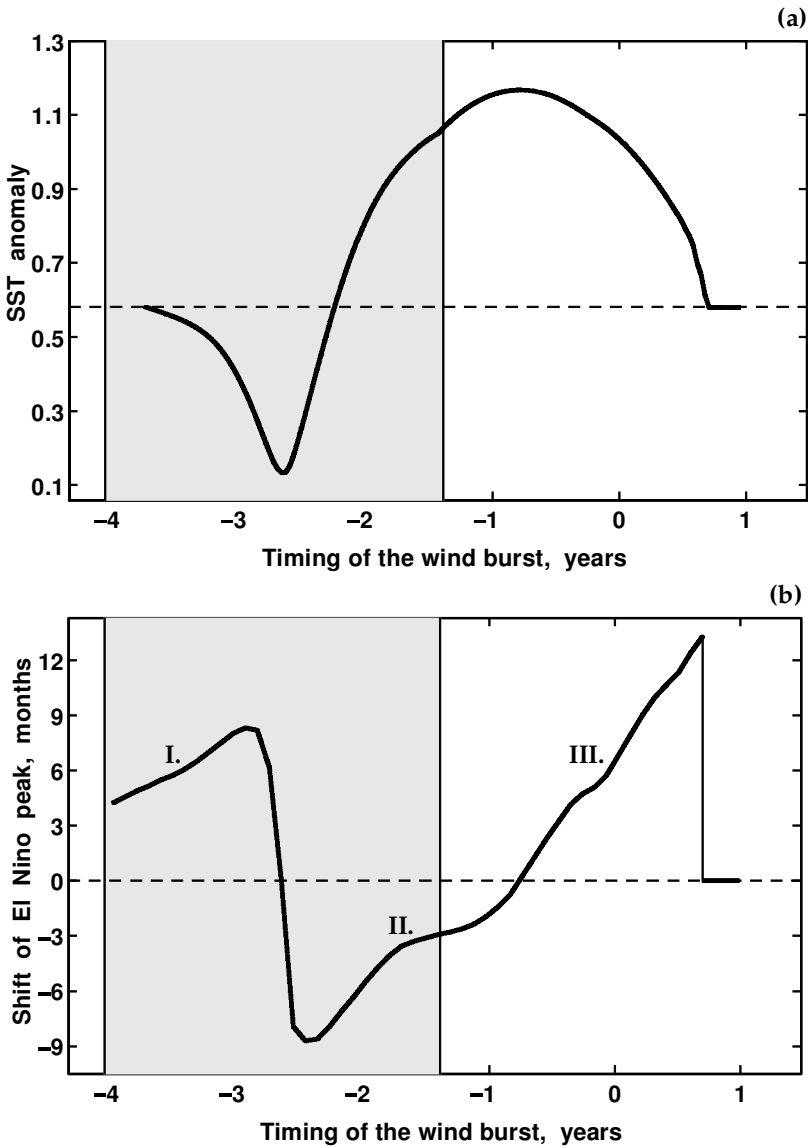


Figure 12. (a) The impact, on the magnitude of El Niño, of westerly wind bursts (WWBs) that happen at different times of one cycle of a pre-existing southern oscillation (SO). The vertical axis displays the strength of the warming of the eastern Pacific Ocean (in degC), while the horizontal axis shows the timing of the bursts within this cycle. Time zero corresponds to the instance when El Niño would have its peak in the absence of the wind bursts. Negative (positive) times correspond to the times before (after) such a peak. The simulated SO has approximately a 5-year period. The magnitude of El Niño in the absence of the wind bursts is shown by the dashed line. The strongest warming develops when a WWB occurs 6–10 months before the peak of El Niño. Shading indicates times when the burst occurs during the cold phase of the cycle, i.e. La Niña. (b) The impact, on the timing of El Niño, of WWBs that happen at different times of a pre-existing SO cycle. The vertical axis displays the shift of the peak of El Niño in time, i.e. its delay (positive values) or its advancement in time (negative values), while the horizontal axis is as in (a). In the absence of the wind bursts, El Niño would peak at time 0. Shading indicates times when the burst occurs during the cold phase of the cycle, i.e. La Niña. See the text for the significance of the regions I, II, and III of the graph.

A further illustration of the impact of WWBs at different times of a cycle is available in Fig. 12(a) whose horizontal time axis covers a complete cycle of the SO (say, the cycle comprised between the arrows in Fig. 11). In the figure, timing 0 corresponds to the peak of El Niño in the absence of any WWB; the negative and positive values of timing indicate the times before and after the peak. The horizontal dashed line is the maximum anomalous temperature in the absence of WWBs, as measured by SST in the eastern equatorial Pacific. The black line shows the maximum temperature reached in response to a WWB. The plot indicates that the strongest warming develops when the WWB occurs at approximately 6 to 10 months in advance of the upcoming El Niño (this conclusion will hold regardless of the strength of the burst).

The results in Fig. 12(a) suggest that in 1997/98 (and probably in 1982/83 too) a weak El Niño was developing when a sequence of WWBs between December 1996 and May 1997 significantly amplified the warm event, so that it became the strongest in the century. Several numerical models succeeded in simulating the onset and development of this El Niño a posteriori, but required that a winter–spring wind burst be specified in order to reproduce the correct amplitude and timing of El Niño (e.g. Perigaud and Cassou 2000; Krishnamurti *et al.* 2000).

Another important effect of the WWBs is to shift the peak of El Niño in time, as shown in Fig. 12(b). The graph in Fig. 12(b) can be divided into three different regions (I, II, and III) in which the delay or advancement of El Niño has different physical explanations. In region I, the burst occurs before the peak of La Niña and leads to a transient warming in the middle of La Niña as discussed in one of the examples in section 4. The extra time the system stays in the La Niña state leads to the delay of the following El Niño. For region II, the burst happens sometime before El Niño and results in accelerating the onset of the warming. For region III, wind bursts happen almost in phase with El Niño or slightly later, leading to the appearance of the second but larger peak of El Niño, the time of which is registered in Fig. 12(b). When the amplitude of the secondary peak becomes smaller than that of the first peak, it is considered that there is no change in the timing of El Niño. It is significant that the two points of the plot where the lag is zero (i.e. with no change in the timing of El Niño) correspond to the times of the strongest and weakest warming in Fig. 12(a).

Further, Fig. 12(b) implies that, by delaying or accelerating the onset of El Niño, WWBs may be able to interfere with the regular phase-locking of El Niño to the seasonal cycle (a canonical El Niño peaks by November–December of the calendar year, see Wallace *et al.* (1998), Tziperman *et al.* (1995) and Jin *et al.* (1996)). There are indications (Wallace *et al.* 1998; Neelin *et al.* 2000) that this regular phase-locking can vary for actual events. For example, in the 1980s and 1990s several El Niño events reached their largest amplitudes in May. Whether the WWBs contribute, in fact, to such variations in the phase-locking remains to be seen. (Also note that some of the quantitative results of Fig. 12 may depend on the relative strength of the wind burst and the particular model used.)

5. DISCUSSION AND CONCLUSIONS

This paper describes how two factors influence the response of the tropical ocean–atmosphere system to westerly wind bursts (WWBs): (1) the background state of the system, and (2) the timing of the burst with respect to the phase of the continual southern oscillation (SO).

These two factors can contribute significantly to the differences between one El Niño and another, and to the modulation of the SO—gradual changes in its period, spatial structure, etc. Certain background conditions—specific combinations of the mean (zonally and temporally averaged) wind intensity τ and mean depth of the thermocline H —are shown to be optimal to ensure a large warming of the eastern Pacific after a WWB.

The deepening of the thermocline, and the weakening of the easterly winds, from the cold '60s and '70s to the warmer '80s and '90s, appears to have increased the sensitivity of the system to the wind bursts. This happened because those winds are confined to the neighbourhood of the date-line, and thus affect developments further east by their effect on vertical movements of the thermocline. This means that their influence should be prominent when modes of the 'delayed oscillator' type (or 'remote' type) are favoured. That has been the case since the 1980s.

Since that time, an SO with a period close to 5 years, appears to have been present continually (see Fig. 1). In this study it has been shown that the phase of this oscillation determines the particular impact of WWBs at different times (in the same way that the phase of a swinging pendulum determines the impact of random blows always in the same direction). Only the bursts that happen about 6 to 10 months before El Niño will have a major impact and significantly increase its intensity. That was probably the case in 1982 and 1997. Nonlinear effects, not described in our model, may have further amplified the warming—in a sequence of WWBs during the onset of El Niño each consecutive wind burst is able to penetrate farther east, thus increasing the overall impact on the ocean–atmosphere system. The wind bursts that happen during the cold phase of the cycle have either negligible or negative impact on the up-coming El Niño.

From inspecting Fig. 1, it is clear that each El Niño is distinct and can be enormously different from others. It has been shown that the WWBs are able to contribute significantly to these differences between one El Niño and the next by subtracting or adding energy to the SO. A WWB can strengthen or weaken El Niño, or it can delay El Niño or accelerate the onset of warming. A burst can lead to a brief, transient warming during La Niña, or to El Niño with several peaks. It is a complex interplay between the natural modes of oscillation, random wind disturbances in the form of the bursts, and the decadal fluctuation of the mean state that contribute significantly to the irregularity of the SO in Fig. 1. The simple model used, although too crude to describe the real system in its full complexity, serves here to illustrate various aspects of such interplay.

This study bridges two different approaches towards El Niño and the SO. In one approach the tropical ocean–atmosphere interactions are considered to be inherently unstable, and to give rise to a continual oscillation (as in the classical delayed-oscillator). If the system is marginally stable or moderately damped, the addition of atmospheric noise sustains a continual oscillation (e.g. Blanke *et al.* 1997; Kirtman and Schopf 1998). In the alternative approach, El Niño evolves through the rapid growth of a sufficiently strong perturbation, and is described mathematically in terms of an initial-value problem (e.g. McPhaden and Yu 1999). As shown here, these two descriptions are not in opposition. At certain times one description will be more appropriate than another, but both are needed to describe and predict El Niño.

These results have important implications for the interpretation of the response of coupled GCMs of the ocean and atmosphere to WWBs. Depending on the background state simulated by a model, it can be more or less sensitive to WWBs. Consider, for example, El Niño of 1997/98 in the coupled GCM of the European Centre for Medium-range Weather Forecasts (ECMWF). In January of 1997 that model predicted a significant rise in the temperatures of the eastern Pacific similar to what was actually observed during the early months of that year. In April of 1997, however, after assimilation of the

oceanic and atmospheric data that described the impact of a sequence of WWBs, the model failed to anticipate the observed rapid rise in temperatures. Instead, the model predicted only a moderate temperature increase and then the saturation of El Niño. It appears that the model was unable to reproduce the ocean–atmosphere interactions in response to the WWBs, and the part of the evolution of El Niño that critically depended on the bursts, possibly because of the relatively strong cold climate drift of the ECMWF model. That drift corresponds to a shift in the mean state of the model towards point B or even towards point E of Fig. 3—a move associated with decreased sensitivity to WWBs.

This consideration suggests a useful tool for diagnosing coupled GCMs that does not require prolonged calculations of several cycles of the SO: one should introduce an external forcing in the form of a WWB into the GCM, and then inspect the response of the model to this burst under different combinations of the model's parameters (e.g. mixing, cloud parametrization, etc.). In another approach, after initializing a GCM with the data from observations, and superimposing a WWB, one can test the response of the current state of the ocean–atmosphere to such forcing. This may supplement the usual predictability studies, in which the model is run for 3, 6, 9 or more months, and the results are compared with subsequent observations.

A recent analysis of 12 statistical and dynamical models used for El Niño predictions, by Landsea and Knaff (2000), finds that at the long (1–2 years) and even medium (6–11 months) ranges there were 'no models that provided useful and skillful forecasts for the entirety of the 1997–1998 El Niño'. At the medium range no models were able to anticipate even one half of the actual amplitude of the peak of El Niño. Most of the models were wrong in predicting the timing of the onset and/or demise of El Niño, and unable to predict the full duration time of the event. If the WWBs of early 1997 were indeed partially responsible for the large amplitude and other characteristics of the 1997–1998 El Niño, then this result is not surprising. Prediction of the observed intensity of El Niño would have required the prediction of the occurrence of WWBs, a phenomenon that at present is regarded to occur at random.

The effect of easterly wind bursts (EWBs) over the western Pacific on the coupled system goes beyond the scope of the present paper. A study of the rectified effect on the ocean of a sequence of alternating EWBs and WWBs has been completed by Kessler and Kleeman (2000). A work on the rectified effects based on our coupled model will be presented elsewhere. In general, it appears that EWBs are less important than WWBs because they produce cold temperature anomalies in the eastern Pacific, which, in turn, can induce only relatively weak wind anomalies. The time the EWBs may matter the most is during El Niño—it has been suggested that the demise of El Niño of 1997/98 was influenced by an EWB (Takayabu *et al.* 1999). It is still unclear, however, to what extent that easterly burst accelerated the onset of a La Niña event which, as seen in the subsurface data, was approaching anyhow.

ACKNOWLEDGEMENTS

This research was supported by the National Oceanic and Atmospheric Administration under contract NA86GP0338, and the National Aeronautics and Space Administration under contract 1229832. The author is grateful to A. Rosati, M. Harrison, S. Harper, M. McPhaden, D. Anderson, T. Stockdale, an anonymous reviewer, and especially to George Philander who inspired this study, Julia Slingo for her helpful comments and support and Barbara Winter and Andrew Wittenberg who read thoroughly several drafts of the paper.

APPENDIX

The APE balance in the model

The ocean dynamics in the model is described by the linear shallow-water equations on the equatorial β -plane in the long-wave approximation. For simplicity, symmetry with respect to the equator, and no annual forcing are assumed:

$$u_t + g'h_x - \beta yv = -ru + \widehat{\tau}/\rho d, \quad (\text{A.1})$$

$$h_t + H(u_x + v_y) = -rh, \quad (\text{A.2})$$

$$g'h_y + \beta yu = 0. \quad (\text{A.3})$$

The notation is conventional with positive $h(x, y, t)$ denoting the total local depth of the thermocline, $u(x, y, t)$ the zonal velocity, $v(x, y, t)$ the meridional velocity, $\widehat{\tau}(x, y, t)$ the zonal wind stress, d the depth characterizing the effect of wind on the thermocline, ρ the mean water density, H the mean depth of the thermocline, r the linear Raleigh damping, and g' the reduced gravity. The standard no-flow boundary condition is applied at the eastern ocean boundary, and the no-net-flow condition at the western boundary of the basin (e.g. Jin and Neelin 1993).

The wind stress $\widehat{\tau}$ is split into the mean (time-averaged) part $\overline{\tau}(x, y)$ and the perturbation $\tau'(x, y, t)$. Hereafter, the overbars and primes denote mean and anomalous values, respectively (except in g'):

$$\widehat{\tau} = \overline{\tau} + \tau'. \quad (\text{A.4})$$

The local (time-averaged) thermocline slope on the equator is related to $\overline{\tau}$ through the approximate balance:

$$g'\overline{h}_x \approx \overline{\tau}/\rho d. \quad (\text{A.5})$$

The mean wind intensity τ used in the main part of this paper is actually proportional to the zonally-averaged $\overline{\tau}$ on the equator. The wind-stress perturbation τ' is related to the SST anomaly $T' = T'(x, t)$ through a simplified Gill-type atmosphere, in which

$$\tau' = \mu A(x, y, T'), \quad (\text{A.6})$$

where $A(x, y, T')$ is a linear integral operator, and μ is the nondimensional coupling strength. $\mu = 0$ implies that there is no coupling between the ocean and atmosphere; $\mu = 0.9$ is chosen as the standard coupling. (For further details of the model see Fedorov and Philander (2001), also Jin and Neelin (1993).) The effect of WWBs is included in the equations by adding τ_{wwb} to the right-hand side of (A.6).

Adding (A.1) multiplied by u , and (A.2) multiplied by h , and using (A.3) and (A.4) with the boundary conditions, one can easily derive the balance equation for the perturbation energy E of the system:

$$E_t + 2rE = \kappa \iint (\overline{u}\tau' + u'\overline{\tau} + u'\tau') dx dy, \quad (\text{A.7})$$

where

$$E = \rho \iint \left(\frac{g'h^2}{2} + \frac{Hu^2}{2} \right) dx dy - \rho \iint \left(\frac{g'\overline{h}^2}{2} + \frac{H\overline{u}^2}{2} \right) dx dy, \quad (\text{A.8})$$

and the integrals are calculated over the tropical Pacific Ocean (130°E–85°W, 15°S–15°N). (The factor $\kappa = H/d$ reflects the difference of the vertical structure of the ocean

from that used in the single-layer shallow-water models. Once $d = H$, then $\kappa = 1$, and the right-side of Eq. (A.7) conforms to the conventional definition of the wind power.)

Since the perturbation kinetic energy of the motion under consideration is very small (in our calculations it was of the order of several per cent of the total; for a reference see Goddard and Philander (2000)), Eqs. (A.7) and (A.8) can be rewritten with a good accuracy as

$$E_t = W + (\dots) \quad (\text{A.9})$$

$$E = \frac{\rho}{2} \iint g' h^2 dx dy - \frac{\rho}{2} \iint g' \bar{h}^2 dx dy, \quad (\text{A.10})$$

$$W = \kappa \iint (\bar{u}\tau' + u'\bar{\tau}) dx dy, \quad (\text{A.11})$$

where E is now the APE of the system oscillations and W is the linearized wind power, i.e. the work done by the wind per unit time. The omitted terms in the brackets describe the higher-order nonlinear terms (negligible for small perturbations), explicit energy dissipation, the energy loss at the western, northern and southern boundaries, and any numerical dissipation after finite-differencing. Equations (A.9)–(A.11) represent the fact that the only way one can change the total APE of the system is through the work of the wind or through dissipation. Note that (A.10) defines the APE with respect to the mean state of the coupled ocean–atmosphere rather than with respect to the hydrostatically balanced reference state with no zonal and meridional dependences. As such, it can be both positive and negative. The expression for the APE can be further linearized to yield

$$E = \rho g' \iint h' \bar{h} dx dy. \quad (\text{A.12})$$

REFERENCES

- | | | |
|--|------|--|
| Battisti, D. S. | 1988 | Dynamics and thermodynamics of a warming event in a coupled tropical atmosphere–ocean model. <i>J. Atmos. Sci.</i> , 45 , 2889–2919 |
| Battisti, D. S. and Hirst, A. C. | 1989 | Interannual variability in a tropical atmosphere ocean model— influence of the basic state, ocean geometry and nonlinearity. <i>J. Atmos. Sci.</i> , 46 , 1687–1712 |
| Blanke, B., Neelin, J. D. and Gutzler, D. | 1997 | Estimating the effect of stochastic wind stress forcing on ENSO irregularity. <i>J. Climate</i> , 10 , 1473–1486 |
| Boulanger, J. P. and Menkes, C. | 1995 | Propagation and reflection of long equatorial waves in the Pacific Ocean during the 1992–1993 El Niño. <i>J. Geophys. Res.</i> , 100 , 25041–25059 |
| Cane, M. A., Zebiak, S. E. and Dolan, S. C. | 1986 | Experimental forecasts of El Niño. <i>Nature</i> , 321 , 827–832 |
| Chang, P., Ji, L., Li, H. and Flugel, M. | 1996 | Chaotic dynamics versus stochastic processes in El Niño–Southern oscillation in coupled ocean–atmosphere models. <i>Physica D</i> , 98 , 301–320 |
| Chao, Y., Li, X., Ghil, M. and McWilliams, J. C. | 2000 | Pacific interdecadal variability in this century’s sea surface temperatures. <i>Geophys. Res. Lett.</i> , 27 , 2261–2264 |
| Delcroix, T., Boulanger, J. P., Masia, F. and Menkes, C. | 1994 | Geosat-derived sea level and surface current anomalies in the equatorial Pacific during the 1986–1989 El Niño and La Niña. <i>J. Geophys. Res.</i> , 99 , 25093–25107 |
| Farrell, B. F. and Moore, A. M. | 1992 | An adjoint method for obtaining the most rapidly growing perturbation to oceanic flows. <i>J. Phys. Oceanogr.</i> , 22 , 338–349 |
| Fedorov, A. V. and Philander, S. G. H. | 2000 | Is El Niño changing? <i>Science</i> , 288 , 1997–2002 |
| | 2001 | A stability analysis of the tropical ocean–atmosphere interactions (Bridging the measurements of, and the theory for, El Niño). <i>J. Climate</i> , 14 , 3086–3101 |

- Giese, B. S. and Carton, J. A. 1999 Interannual and decadal variability in the tropical and midlatitude Pacific Ocean. *J. Climate*, **12**, 3402–3418
- Giese, B. S. and Harrison, D. E. 1991 Eastern equatorial Pacific response to 3 composite westerly wind types. *J. Geophys. Res.*, **96**, 3239–3248
- Goddard, L. and Graham, N. E. 1997 El Niño in the 1990s. *J. Geophys. Res.*, **102**, 10423–10436
- Goddard, L. and Philander, S. G. H. 2000 The energetics of El Niño and La Niña. *J. Climate*, **13**, 1496–1516
- Guilderson, T. P. and Schrag, D. P. 1998 Abrupt shift in subsurface temperatures in the Tropical Pacific associated with changes in El Niño. *Science*, **281**, 240–243
- Harrison, D. E. and Giese, B. S. 1988 Remote westerly wind forcing of the eastern equatorial Pacific; some model results. *Geophys. Res. Lett.*, **15**, 804–807
- Harrison, D. E. and Vecchi, G. A. 1997 Westerly wind events in the tropical Pacific, 1986–95. *J. Climate*, **10**, 3131–3156
- Hendon, H. H. and Glick, J. D. 1997 Intraseasonal air–sea interaction in the tropical Indian and Pacific Oceans. *J. Climate*, **10**, 647–661
- Hendon, H. H., Liebmann, B. and Glick, J. D. 1998 Oceanic Kelvin waves and the Madden–Julian oscillation. *J. Atmos. Sci.*, **55**, 88–101
- Jin, F. F. 1997a An equatorial ocean recharge paradigm for ENSO. 1. Conceptual model. *J. Atmos. Sci.*, **54**, 811–829
- 1997b An equatorial ocean recharge paradigm for ENSO. 2. A stripped-down coupled model. *J. Atmos. Sci.*, **54**, 830–847
- Jin, F. F. and Neelin, J. D. 1993 Modes of interannual tropical ocean–atmosphere interaction—a unified view. Part I: Numerical results. *J. Atmos. Sci.*, **50**, 3477–3503
- Jin, F. F., Neelin, J. D. and Ghil, M. 1996 El Niño–Southern Oscillation and the annual cycle—subharmonic frequency-locking and aperiodicity. *Physica D*, **98**, 442–465
- Kessler, W. S. and Kleeman, R. 2000 Rectification of the Madden–Julian oscillation into the ENSO cycle. *J. Climate*, **13**, 3560–3575
- Kessler, W. S. and McPhaden, M. J. 1995 Oceanic equatorial waves and the 1991–93 El Niño. *J. Climate*, **8**, 1757–1774
- Kessler, W. S., McPhaden, M. J. and Weickmann, K. M. 1995 Forcing of intraseasonal Kelvin waves in the equatorial Pacific. *J. Geophys. Res.*, **100**, 10613–10631
- Kindle, J. C. and Phoebus, P. A. 1995 The ocean response to operational westerly wind bursts during the 1991–1992 El Niño. *J. Geophys. Res.*, **100**, 4893–4920
- Kirtman, B. P. and Schopf, P. S. 1998 Decadal variability in ENSO predictability and prediction. *J. Climate*, **11**, 2804–2822
- Krishnamurti, T. N., Bachiochi, D., LaRow, T. E. and Jha, B. 2000 Coupled atmosphere–ocean modeling of the El Niño of 1997–98. *J. Climate*, **13**, 2428–2459
- Landsea, C. W. and Knaff, J. A. 2000 How much skill was there in forecasting the very strong 1997–98 El Niño? *Bull. Am. Meteorol. Soc.*, **81**, 2107–2119
- McPhaden, M. J. 1999 Climate oscillations—Genesis and evolution of the 1997–98 El Niño. *Science*, **283**, 950–954
- McPhaden, M. J. and Yu, X. 1999 Equatorial waves and the 1997–98 El Niño. *Geophys. Res. Lett.*, **26**, 2961–2964
- Madden, R. A. and Julian, P. R. 1972 Description of global-scale circulation cells in the tropics with a 40–50 day period. *J. Atmos. Sci.*, **28**, 1109–1123
- 1994 Observations of the 40–50 day tropical oscillation—a review. *Mon. Weather Rev.*, **122**, 814–837
- Moore, A. M. and Kleeman, R. 1997 The singular vectors of a coupled ocean–atmosphere model of ENSO. 1: Thermodynamics, energetics and error growth. *Q. J. R. Meteorol. Soc.*, **123**, 953–981
- 1999 Stochastic forcing of ENSO by the intraseasonal oscillation. *J. Climate*, **12**, 1199–1220
- Neelin, J. D., Jin, F. F. and Syu, H.-H. 2000 Variations in ENSO phase locking. *J. Climate*, **13**, 2570–2590
- Penland, C. and Sardeshmukh, P. D. 1995 The optical growth of tropical sea surface temperature anomalies. *J. Climate*, **8**, 1999–2024
- Perigaud, C. M. and Cassou, C. 2000 Importance of oceanic decadal trends and westerly wind bursts for forecasting El Niño. *Geophys. Res. Lett.*, **27**, 389–392
- Philander, S. G. H. 1981 The response of equatorial oceans to a relaxation of the trade winds. *J. Phys. Oceanogr.*, **11**, 76–89
- Roulston, M. S. and Neelin, J. D. 2000 The response of an ENSO model to climate noise, weather noise and intraseasonal forcing. *Geophys. Res. Lett.*, **27**, 3723–3726
- Schopf, P. S. and Suarez, M. J. 1988 Vacillations in a coupled ocean–atmosphere model. *J. Atmos. Sci.*, **45**, 549–566

- Slingo, J. M., Rowell, D. P., Sperber, K. R. and Nortley, F. 1999 On the predictability of the interannual behaviour of the Madden-Julian Oscillation and its relationship with El Niño. *Q. J. R. Meteorol. Soc.*, **125**, 583–609
- Takayabu, Y. N., Iguchi, T., Kachi, M., Shibata, A. and Kanzawa, H. 1999 Abrupt termination of the 1997–98 El Niño in response to a Madden-Julian oscillation. *Nature*, **402**, 279–282
- Thompson, C. J. and Battisti, D. S. 2000 A linear stochastic dynamical model of ENSO. Part I: Mode development. *J. Climate*, **13**, 2818–2832
- Trenberth, K. E. and Hoar, T. J. 1996 The 1990–1995 El Niño–Southern Oscillation event—longest on record. *Geophys. Res. Lett.*, **23**, 57–60
- Tziperman, E. M., Cane, M. A. and Zebiak, S. E. 1995 Irregularity and locking to the seasonal cycle in an ENSO prediction model as explained by the quasi-periodicity route to chaos. *J. Atmos. Sci.*, **50**, 293–306
- Vecchi, G. A. and Harrison, D. E. 2000 Tropical Pacific sea surface temperature anomalies, El Niño, and equatorial westerly wind events. *J. Climate*, **13**, 1814–1830
- Wallace, J. M., Rasmusson, E. M., Mitchell, T. P., Kousky, V. E., Sarachik, E. S. and von Storch, H. 1998 The structure and evolution of ENSO-related climate variability in the tropical Pacific: Lessons from TOGA. *J. Geophys. Res.*, **103**, 14241–14259
- Woolnough, S. J., Slingo, J. M. and Hoskins, B. J. 2000 The relationship between convection and sea surface temperature on intraseasonal time-scales. *J. Climate*, **13**, 2086–2104
- Wunsch, C. 1999 The interpretation of short climate records, with comments on the North Atlantic and Southern Oscillations. *Bull. Am. Meteorol. Soc.*, **80**, 245–255
- Zebiak, S. E. 1989 On the 30–60 day oscillation and the prediction of El Niño. *J. Climate*, **2**, 1381–1387
- Zebiak, S. E. and Cane, M. A. 1987 A model El Niño–Southern Oscillation. *Mon. Weather Rev.*, **115**, 2262–2278
- Zhang, Y., Wallace, J. M. and Battisti, D. S. 1997 ENSO-like interdecadal variability: 1900–93. *J. Climate*, **10**, 1003–1020